Available online at www.sciencedirect.com
ScienceDirect
Journal of Nuclear Materials 374 (2008) 482–487
journal of nuclear materials
www.elsevier.com/locate/jnucmat

Texture, residual strain, and plastic deformation around scratches in alloy 600 using synchrotron X-ray Laue micro-diffraction

M.L. Suominen Fuller [a,*], R.J. Klassen [b], N.S. McIntyre [a], A.R. Gerson [c], S. Ramamurthy [a], P.J. King [d], W. Liu [e]

[a] Surface Science Western, Room G-1, Western Science Centre, The University of Western Ontario, London, Ontario, Canada N6A 5B7
[b] Department of Mechanical and Materials Engineering, Room 3002 Spencer Engineering Building, The University of Western Ontario, London, Ontario, Canada N6A 5B9
[c] Applied Centre for Structural and Synchrotron Studies, Mawson Lakes Campus, University of South Australia, Adelaide, South Australia 5095, Australia
[d] Babcock & Wilcox Canada, 581 Coronation Blvd., Cambridge, Ontario, Canada N1R5V3
[e] Advanced Photon Source, Argonne National Laboratory, 9700 S. Cass Avenue, Argonne, IL 60439, USA

Received 25 April 2007; accepted 5 October 2007

Abstract

Deformation around two scratches in Alloy 600 (A600) was studied nondestructively using synchrotron Laue differential aperture X-ray microscopy. The orientation of grains and elastic strain distribution around the scratches were measured. A complex residual deviatoric elastic strain state was found to exist around the scratches. Heavy plastic deformation was observed up to a distance of 20 μm from the scratches. In the region 20–30 μm from the scratches the diffraction spots were heavily streaked and split indicating misoriented dislocation cell structures.

1. Introduction

Pressurized water reactor (PWR) type nuclear power stations are widely used throughout the world and as the nuclear power stations approach their design life, one of the greatest concerns to the owners/operators is the corrosion of steam generators (SGs) which can occur under several different forms such as pitting, thinning and stress corrosion cracking (SCC) [1]. Nickel-based alloy tubes, such as Alloy 600 (A600), used in most of the older power stations are susceptible to stress corrosion cracking (SCC) [2,3]. In fact, SCC of A600 tubing is the single most important reason that nuclear steam generators (SGs) are replaced. Local mechanical stresses from scratches and dents can result in strains at critical grain intersections leading to enhance initiation of chemical attack.

The degree of plastic deformation around scratches in ductile metals affects the mechanical properties of the metal such as its resistance to wear, fatigue, and stress corrosion cracking (SCC). It has therefore been studied extensively both through experimentation and numerical simulations. Most experimental investigations of the plastic deformation around scratches are performed with techniques that involve some forms of metal removal. However, it is preferable to study the plastic deformation without removing the surrounding bulk metal since the removal process can affect the deformed structure of the metal. Evaluating the plastic zone around the scratch nondestructively also allows the sample to be used for subsequent testing such as fatigue or SCC tests.

A nondestructive 3-D X-ray crystal microscope based on Laue diffraction has recently been developed [4–7]. This differential-aperture X-ray microscopy (DAXM) technique is capable of probing local crystal structure, grain orientation and strain tensors with submicrometre spatial resolution. A wire, acting as a knife edge profiler, is used

* Corresponding author.
E-mail address: mfuller@uwo.ca (M.L. Suominen Fuller).

0022-3115/$ - see front matter © 2007 Elsevier B.V. All rights reserved.
doi:10.1016/j.jnucmat.2007.10.015

to sort Laue diffraction patterns along the penetration direction of the polychromatic X-ray microbeam from a synchrotron. This Laue based technique eliminates the need for sample rotation thus simplifying the spatial mapping below 5 μm and provides a truly 3D probe for nondestructively investigating polycrystalline structures on mesoscopic length scales of 0.1–100 μm.

In this investigation differential aperture X-ray microscopy (DAXM) was used to analyze nondestructively the local crystallographic orientation, residual elastic strain, and plastic deformation around scratches in A600. This alloy is used in heat exchanger tubing in electrical power stations and has been found to be susceptible to failure by SCC [2,3]. It also develops complex intergranular strains during loading. The magnitude of these strains is related to the size and crystallographic orientation of the grains [8]. It is therefore important for understanding the SCC properties of A600 to have a technique to nondestructively evaluate the elastic–plastic strain state and the crystallographic orientation around surface defects, such as scratches, so that the same sample can later be used for SCC testing. The DAXM technique provides this capability [4–7].

The DAXM instrument used in this investigation is located at Beamline 34-ID at the Advanced Photon Source (APS) at Argonne National Laboratories. A schematic diagram of the operation of the instrument is shown in Fig. 1. A high energy polychromatic synchrotron X-ray beam is focused by two Kirkpatrick–Baez (KB) mirrors to 0.5 μm by 0.5 μm and then is directed onto the test sample. The X-ray beam penetrates, and generates detectable Bragg reflections over a distance approximately 60–100 μm in A600. Laue diffraction patterns emanating from the region of the sample in the path of the incident X-ray beam are detected with a CCD camera located at 90° to the incident beam. A 50 μm diameter Pt wire is traversed, in micrometer or sub-micrometer steps, across the face of the sample. Laue diffraction spots are systematically obscured from the CCD by the moving wire. In this manner, it is possible to establish the location in the sample from which an obstructed Laue spot originates. A computer program then collates and reconstructs the Laue diffraction images from each micro-region of the sample material along the path of the X-ray beam. By moving the sample with respect to the incident X-ray beam and at each position, scanning the Pt wire across the sample, the local crystallographic orientation and residual deviatoric strain tensor can be determined with a spatial resolution of about 0.5 μm × 0.5 μm × 1.0 μm [4–7].

2. Experimental

Two A600 coupons (0.050 wt%C, 14.8 wt%Cr, 77.9 wt%Ni and 6.29 wt%Fe) each 2.5 cm × 1.25 cm × 0.6 cm thick, were examined. The as-received coupons were in the mill annealed condition. One surface of each coupon was then mechanically polished to a 0.25 μm surface finish and etched in a Glyceragia solution (10 ml NHO_3, 25 ml HCl, 30 ml Glycerin).

One pass scratch of about 1.5 mm length was made on each of the two etched coupons. A deep scratch having a width $W = 100$ μm and a depth $h = 40$ μm ($W/h = 2.5$), was made with a conical indenter on one coupon, while a

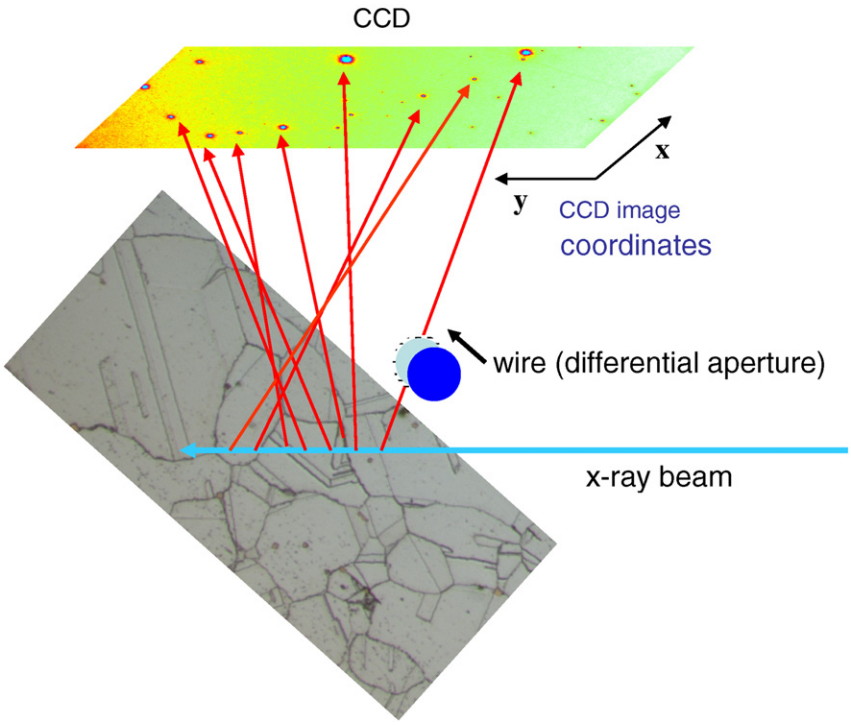

Fig. 1. Schematic of the operation of the DAXM.

shallow scratch, $W = 20$ μm and $h = 1.5$ μm ($W/h = 13.3$) was made with a spherical indenter on the other coupon (Fig. 2).

The residual deviatoric elastic strain components and the crystallographic orientation around each scratch, at approximately the mid-length of the scratch, were analyzed by DAXM. For these experiments, the Pt wire was moved a distance of 399 μm across the scratch and 400 CCD images of the Laue diffraction patterns were recorded at approximately 1 μm intervals of wire movement per image. The sample was then moved in 1 μm and 2 μm steps with respect to the incident X-ray beam in the case of the shallow and the deep scratches, respectively. At each step the Pt wire was scanned across the sample. The CCD detector used in these experiments was a Roper Scientific PI•SCX:4300 camera. The 2084×2084-pixel CCD with an imaging area of 50×50 mm, was placed 50 mm above the sample, and a 4×4 binned mode was used to speed up the data collection. Thus the resulting calculated noise level in the elastic strains from the diffraction data is approximately $\pm 2 \times 10^{-3}$ due to the detector parameters employed. Depth-resolved Laue diffraction spots can be quite streaky, indicating that plastic deformation exists in a 1 μm^3 volume. Heavily streaked Laue images do not get indexed due to difficulty in peak fitting (Fig. 3 (S2-3, D2-3)).

The reconstructed Laue images were indexed and the deviatoric elastic strain tensor $\hat{\varepsilon}_{ij}$ was calculated for each 1 μm^3 volume as (Figs. 4 and 5)

$$\hat{\varepsilon}_{ij} = \begin{bmatrix} \varepsilon_{11} - \delta/3 & \varepsilon_{12} & \varepsilon_{13} \\ \varepsilon_{21} & \varepsilon_{22} - \delta/3 & \varepsilon_{23} \\ \varepsilon_{31} & \varepsilon_{32} & \varepsilon_{33} - \delta/3 \end{bmatrix},$$

where $\delta = \varepsilon_{11} + \varepsilon_{22} + \varepsilon_{33}$.

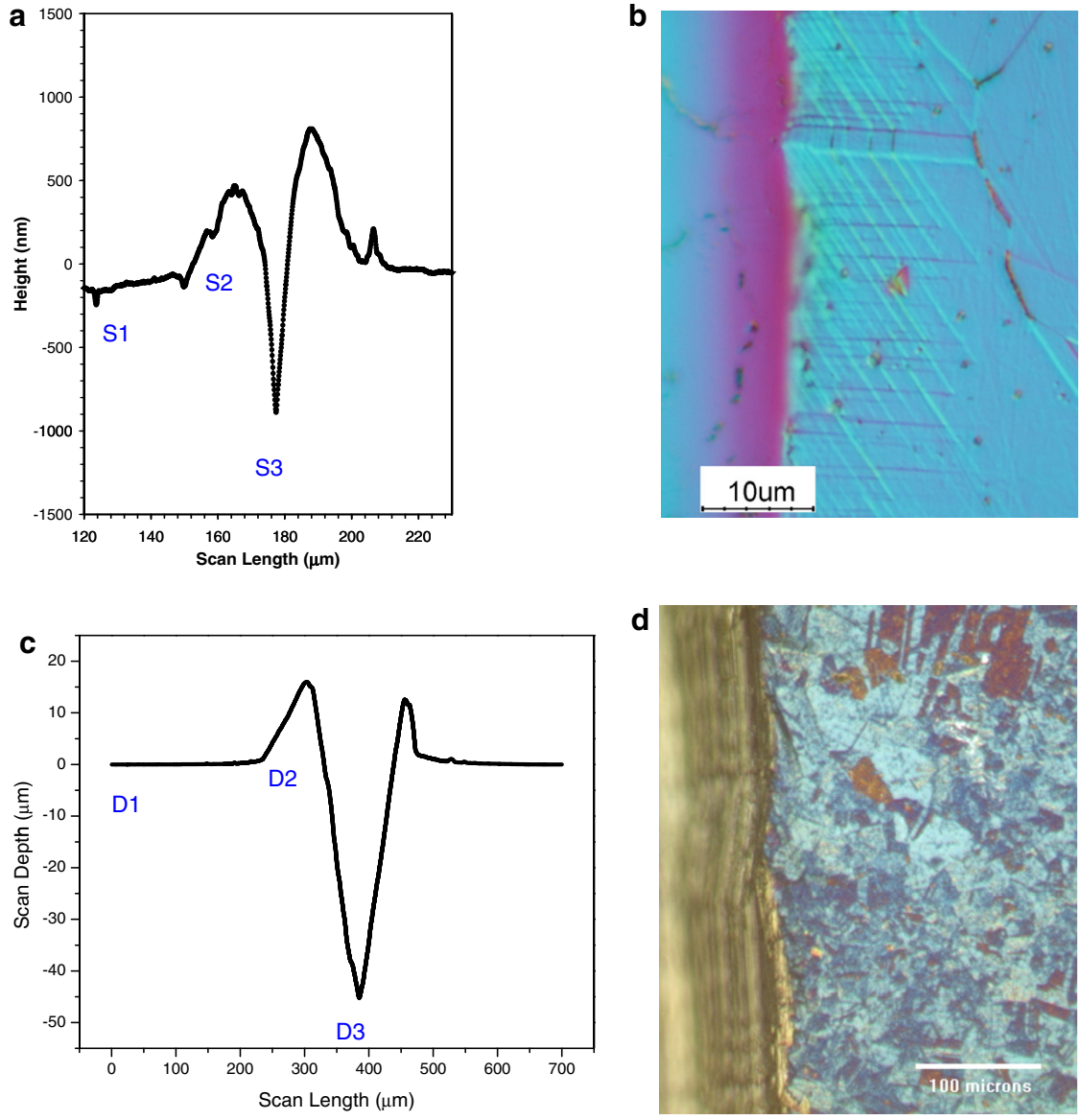

Fig. 2. (a) Profile of the shallow scratch. (b) Optical image showing slip steps near the edge of the shallow scratch. (c) Profile of the deep scratch. (d) Optical image showing slip steps near the edge of the deep scratch.

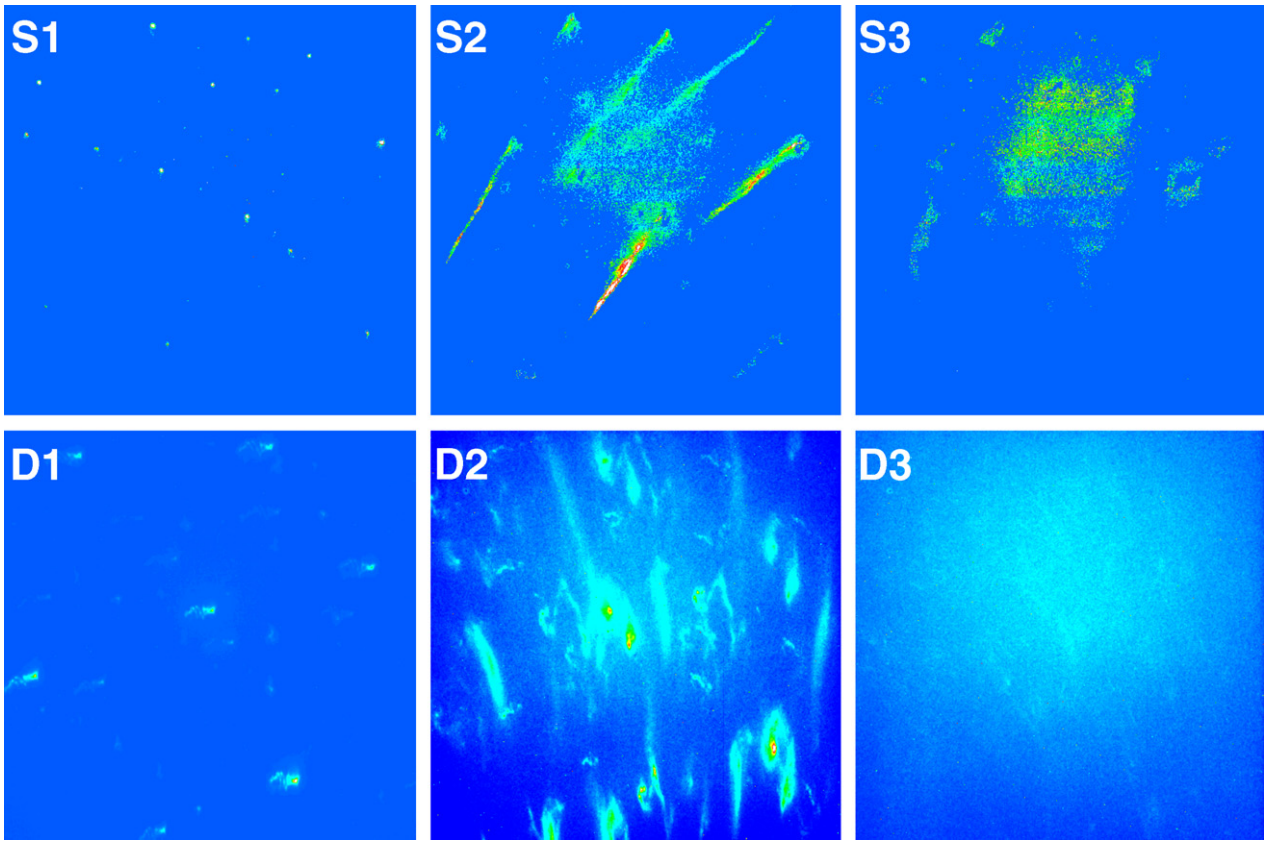

Fig. 3. CCD images from three regions of the shallow (S) and deep (D) scratches. S1 and D1 are from regions away from the scratch, S2 and D2 are from the edge of the scratch, and S3 and D3 are from inside the scratch. The approximate locations of these regions are indicated in the depth profiles of these scratches in Fig. 2(a) and (c).

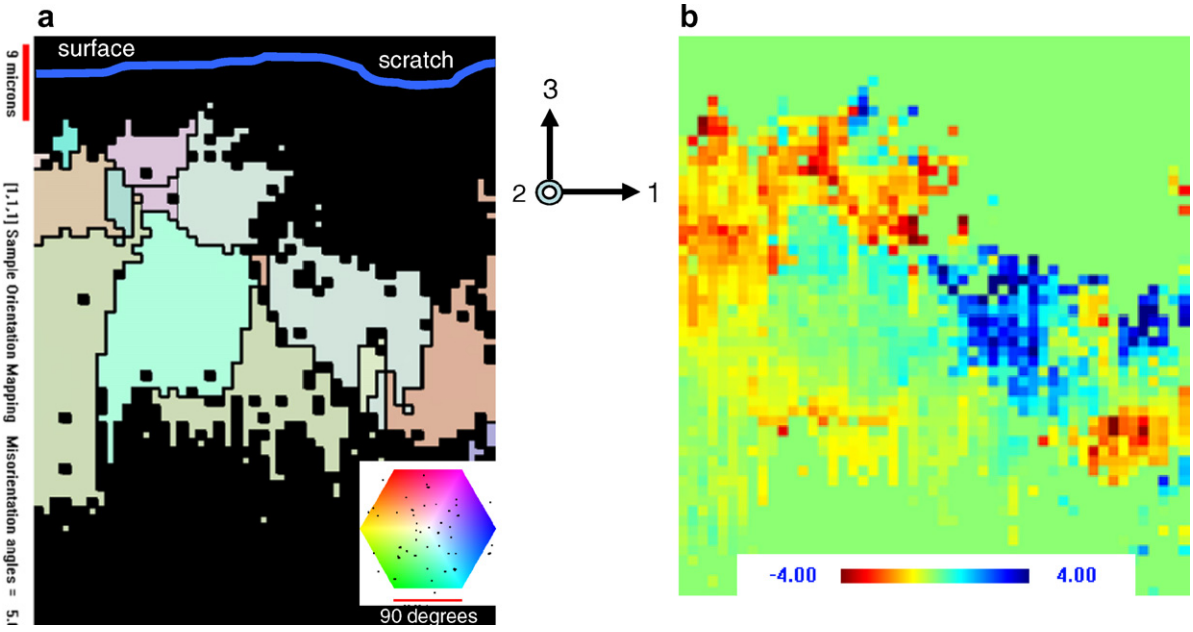

Fig. 4. 2D orientation map of the plane perpendicular to the axial direction of (a) the shallow scratch and (b) 2D map of the $\hat{\varepsilon}_{11}$ (scale $= -4.00 \times 10^{-3}$ to 4.0×10^{-3}) of the shallow scratch on the same plane as in (a).

After the DAXM analysis, the coupon containing the deep scratch was sectioned and a plane normal to scratch was polished and etched to reveal the grain structure (Fig. 6). Please note that the region shown in the

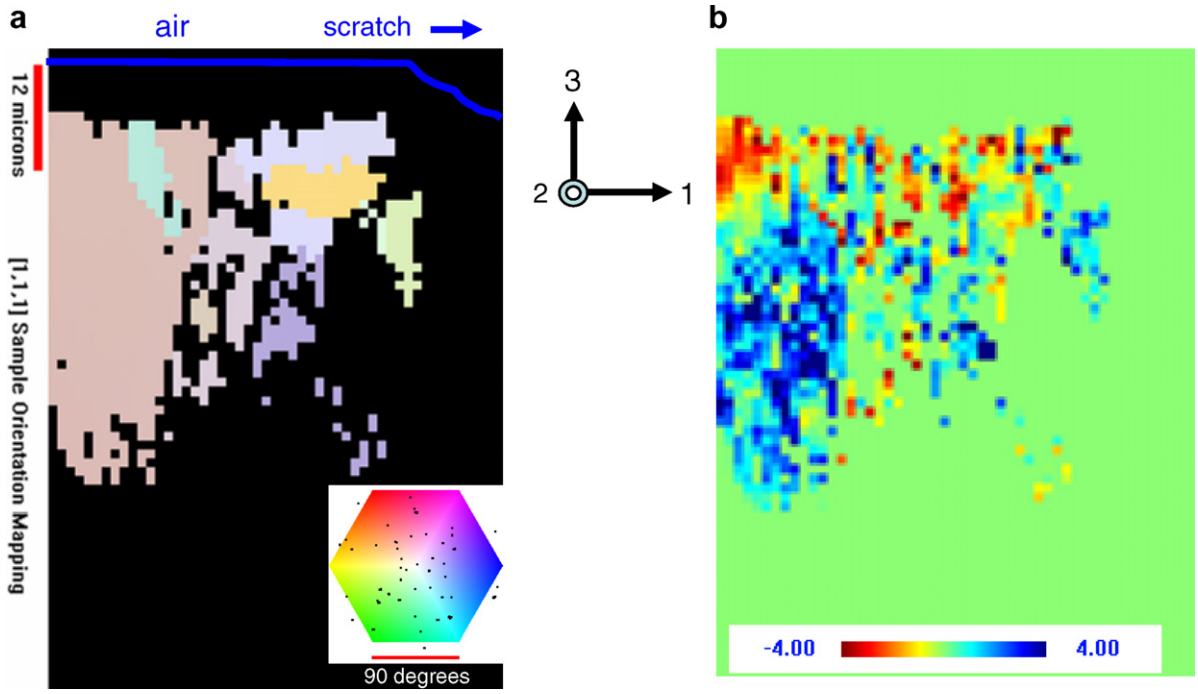

Fig. 5. 2D orientation map of the plane perpendicular to the axial direction of (a) the deep scratch and (b) 2D map of the $\hat{\varepsilon}_{11}$ (scale = -4.00×10^{-3} to 4.0×10^{-3}) of the deep scratch on the same plane as in (a).

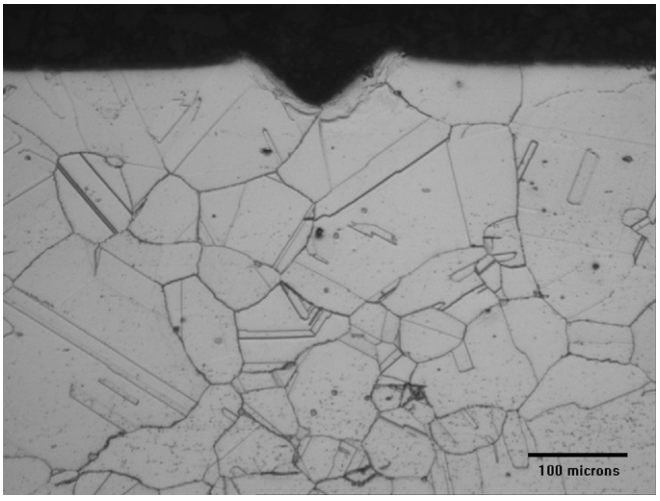

Fig. 6. Optical image of the etched cross-section normal to the axial direction of the deep scratch.

cross-section in Fig. 6 does not correspond to the region represented by the depth-resolved orientation map from the deep scratch shown in Fig. 5(a).

3. Results and discussion

The grain size of the A600, on the plane normal to the length of the scratch but far from the scratch was quite variable with grains ranging from approximately 15 μm to 200 μm (Fig. 6). Deformation of the material under the deep scratch shown in the etched cross-section in Fig. 6 is evident.

Fig. 2(b) and (d) shows the slip planes on the polished surface of the scratched samples. For the deep scratch, the slip steps extend approximately 100–150 μm from the scratch edge while the slip steps for the shallow scratch extend approximately 30 μm from the scratch edge. The width of the slipped region normalized to the width of the scratches is therefore between 1 and 1.5. This is in good agreement with measurements of the width of the plastic zone around scratches in a Cu–Al alloy [9,10].

Laue diffraction patterns from three selected regions of the shallow (S) and deep (D) scratched samples, region 1, away from the scratch, region 2 at the scratch edge and region 3, inside the scratch, are presented in Fig. 3. The approximate locations of these regions are indicated in the depth profiles of the scratches in Fig. 2(a) and (c). The diffraction spots from the region away from the two scratches (S1 and D1), show only moderate streaking, thus indicating only small amounts of plastic deformation. As the scratch is approached, the diffraction spots become progressively more streaked as shown S2 and D2 from the scratch edges. The association of streaked and splitting of Laue diffraction spots with the presence of lattice rotations resulting from geometrically necessary dislocation structures has been documented in detail by Barabash et al. [11–13]. Our observation of streaking and splitting of the Laue diffraction spots indicates that the plastic deformation near scratches made in the A600 at room temperature occurs by the formation of dislocation structures, within the grains, that have high degrees of angular misorientation. This is consistent with previously reported finding of misoriented dislocation structures, of size in

the submicron range, in the near surface areas of copper deformed by scratching and indentation [14,15]. The diffraction patterns from inside the two scratches (S3 and D3) show only diffuse structure indicating that the grain structure around the scratch has been very heavily deformed. This agrees with previously reported findings of 'nanostructured' regions of about 10 nm size directly below the surface of annealed Cu that was heavily deformed by scratching [14].

Figs. 4(a) and 5(a) show the orientation of the [1 1 1] crystallographic direction, with respect to the sample surface normal, around the shallow and the deep scratches, respectively. The location of the scratch is labeled in each map. The blue[1] line on the OM of the shallow scratch indicates the surface. Laue images above this line exhibit no structure. The diffraction patterns from the dark regions around the scratches could not be indexed due to heavy plastic deformation. Both figures indicate that the grains in this material are randomly oriented.

Maps of the magnitude of $\hat{\varepsilon}_{11}$ around the shallow and the deep scratches are shown in Figs. 4(b) and 5(b), respectively. There is considerable residual elastic strain, up to $\hat{\varepsilon}_{11} = 4 \times 10^{-3}$, in the region close to the scratches with the magnitude of $\hat{\varepsilon}_{11}$ decreasing with increasing distance from the scratch. The magnitude of $\hat{\varepsilon}_{11}$ near the scratches varies with grain orientation. These figures indicate that large elastic strain discontinuities exist across the grain boundaries in A600 and their magnitude depends upon the relative misorientation of the adjoining grains and the structure of the grain boundary. This clearly suggests that different grain boundaries in the A600 will have different susceptibilities to SCC.

4. Conclusions

Optical micrographs indicate that the width of the slipped regions in the deep and shallow scratches normalized to the width of the scratches are between 1 and 1.5. Laue diffraction using high energy synchrotron X-rays, shows a high degree of plastic deformation in the scratch region. The diffraction patterns from directly around the scratches show only diffuse structure, indicating that the grain structure in these regions is 'nanostructured' and has been heavily deformed. Moving away from this 'nanostructured' region, the Laue patterns exhibit streaking and splitting indicating misoriented dislocation cell structures.

Elastic strain discontinuities are observed across grain boundaries, away from the scratch region in A600, suggesting that different grain orientations in the vicinity of the scratch have uniquely different strain states and dislocation structures. This suggests therefore that scratches in A600 may have a varying susceptibility to SCC depending upon the crystallographic orientation in the region around a scratch. We are presently investigating this area further.

Acknowledgements

Experiments were performed on the XOR/UNI beamline 34-ID-E at the Advanced Photon Source, Argonne National Lab. Use of the Advanced Photon Source was supported by the US Department of Energy, Office of Science, Office of Basic Energy Sciences, under Contract No. DE-AC02-06CH11357.

The authors gratefully acknowledge the funding contributions from Babcock & Wilcox Canada (BWC) and the Centre for Materials and Manufacturing Ontario and the Department of Innovation, Industry and Regional Development, State of Victoria, Australia. The authors also thank Mr H. Wang, Department of Materials Engineering, University of Western Ontario, for the metallographic preparation and Mr Edward Lehockey of Ontario Power Generation for many useful discussions.

References

[1] P. Berge, Mater. Perform. 36 (1997) 56.
[2] P.M. Scott, F.N. Speller, Corrosion 56 (2000) 771.
[3] L.E. Thomas, S.M. Bruemmer, Corrosion 56 (2000) 572.
[4] B.C. Larson, W.G. Yang, G.E. Ice, J.D. Budai, J.Z. Tischler, Nature 415 (2002) 887.
[5] G.E. Ice, B.C. Larson, Adv. Eng. Mater. 2 (2000) 643.
[6] W. Liu, G.E. Ice, B.C. Larson, W. Yang, J.Z. Tischler, J.D. Budai, Metall. Mater. Trans. A 35 (2004) 1963.
[7] K.-S. Chung, G.E. Ice, J. Appl. Phys. 86 (1999) 5249.
[8] T.M. Holden, C.H. Tomé, R.A. Holt, Metall. Mater. Trans. A 29 (1998) 2967.
[9] S. Kobayashi, T. Harada, S. Miura, J. Mater. Sci. 29 (1994) 26.
[10] S. Kobayashi, M. Kuwata, K. Mori, S. Miura, J. Mater. Sci. 31 (1996) 5797.
[11] R. Barabash, Mater. Sci. Eng. A 309&310 (2001) 49.
[12] R. Barabash, G.E. Ice, B.C. Larson, G.M. Pharr, K.-S. Chung, W. Yang, Appl. Phys. Lett. 79 (2001).
[13] R.I. Barabash, G.E. Ice, F.J. Walker, J. Appl. Phys. 93 (2003) 1457.
[14] D.A. Hughes, N. Hansen, Phys. Rev. Lett. 87 (2001) 135503.1.
[15] Y. Wang, D. Raabe, C. Klüber, F. Roters, Acta Mater. 52 (2004) 2229.

[1] For interpretation of color in Figs. 1–5, the reader is referred to the web version of this article.